Cell Death Mechanisms in a Mouse Model of Retinal Degeneration in Spinocerebellar Ataxia 7

Cecile Lebon, Francine Behar-Cohen, Alicia Torriglia

Cell death mechanisms in a mouse model of retinal degeneration in Spinocerebellar ataxia 7

Cecile Lebon[1,2,3], Francine Behar-Cohen[1,2,3] and Alicia Torriglia[1,2,3]

[1]Inserm U1138. Centre des Recherches des Cordeliers, 15, rue de l'Ecole de Médecine, 78006 Paris, France.

[2] Université Pierre et Marie Curie.

[3] Université Paris Descartes.

Correspondingauthor: Alicia Torriglia, alicia.torriglia@inserm.fr

Keywords: Spinocerebellarataxia type 7, retina, caspase-independentcelldeath, polyglutaminedisorder, photoreceptors, toxicity, autophagy, unfoldedproteinresponse.

Abstract:

Spino-cerebellar ataxia type 7 (SCA7) is a polyglutamine (polyQ) disorder characterized by neurodegeneration of the brain, cerebellum,and retina caused by a polyglutamine expansion in ataxin 7.The presence of an expanded polyQ tract in a mutant protein is known to induce protein aggregation, cellular stress, toxicity, and finally cell death. However, the consequences of the presence of mutant ataxin7 in the retina and the mechanisms underlying photoreceptor degeneration remain poorly understood. In this study, we show that in a retinal SCA7 mouse model, polyQ ataxin7 induces stress within the retina and activates Muller cells. Moreover, Unfolded Protein Response and autophagy are activated in SCA7 photoreceptors. We have also shown that the photoreceptor death does not involve a caspase-dependent apoptosis but instead involves apoptosis inducing factor (AIF) and Leukocyte Elastase Inhibitor (LEI/L-DNase II). When these two cell death effectors are downregulated by their siRNA, a significant reduction of photoreceptor death is observed. These results highlight the consequences of polyQ protein expression in the retina and the role of caspase-independent pathways involved in photoreceptor cell death.

Highlights:

The cell death in SCA7 mice model is caspase-independent

The effectors of cell death in the SCA7 mice model are LEI/L-DNase II and AIF

The activation of these effectors result in a TUNEL negative cell death

Introduction

Spinocerebellar ataxia type 7 (SCA7) belongs to the heterogeneous family of neurodegenerative disorders. Clinically, SCA7 is characterized by a progressive ataxia and a gradual vision loss leading to blindness. It is a rare disease caused by an unstable CAG expansion in the *ATXN7* gene leading to the expression of ataxin7 with an abnormal polyglutamine tract (polyQ) (David G et al., 1997). Nine polyQ neurodegenerative disorders have been described so far, including SCA1, SCA2, SCA6, SCA7, SCA 17, Huntington's disease, spinal and bulbar muscular atrophy (SBMA) and dentatorubralpallidoluysian atrophy (DRPLA). The particularity of SCA7, in addition to its great instability of the CAG-repeat length, is the fact that it affects not only brainstem and cerebellum but also leads to retinal degeneration (Michalik A et al., 2004).

The protein encoded by the ATXN7 gene is ubiquitously expressed. It is a subunit of two transcriptional repressor complexes: STAGA (SPT3/TAF9/GCN5) and TFTC (TAF-containing complex) involved in chromatin remodeling and histone acetylation. While the normal range of CAG repeats is under 35, pathological alleles contains 36 repeats and over (Garden GA and La Spada AR, 2008). Like most polyQ disorders, CAG-repeat length is directly correlated to the age of onset and the disease progression: the longer the CAG repeat, the earlier the symptoms appear and the quicker the degeneration occurs (Michalik A,Martin J and Van Broeckhoven C, 2004). Moreover, SCA7 family studies demonstrate a genetic anticipation: the CAG length tends to expand through generations (Garden GA and La Spada AR, 2008). SCA7 patients present with a loss of neuronal cells in the cerebellum and degeneration of photoreceptors in the retina. This degeneration affects cones first but progressesto encompass the entire retina, leading to a cone-rode dystrophyand complete blindness (Michalik A,Martin J and Van Broeckhoven C, 2004). However, the mechanisms of photoreceptor cell death due to the expression of polyQ ataxin7 remain poorly understood.

SCA7 R7E transgenic mice were used to study the retinal degeneration induced by polyQ toxicity. These mice express the human ataxin7 with a 90 glutamines expansion under the rhodopsin promoter (Yvert G et al., 2000). Previous studies have shown that despite the

loss of visual function with aging, these mice show a slow photoreceptor degeneration without a complete loss of the retinal structure (Helmlinger D et al., 2004).

Rod photoreceptors die through different cell death mechanisms including apoptotic and non-apoptotic cell death that remain to be elucidated, and can also show morphological transformation and even cell division (Yefimova MG et al., 2010). In this study, we investigate the molecular pathways of cell death in the SCA7 R7E mouse.

Experimental Procedures

SCA7 mice genotyping

The SCA7 R7E mice line was kindly provided by Dr. Yvon Trottier from IGBMC, Illkirch, France. They have been engineered on a C57/Bl6 background by Jean-Louis Mandel's team.

The mice were maintained in the Ecole Vétérinaire of Maison-Alfort's animal facilities (ENVA). Identification, biopsies and genotyping were performed at PN2 weeks (post-natal). DNA was extracted according to the manufacturer's specifications with the Kapa Express Extract kit (Kapabiosystems). A PCR was then performed with the Kapa2G Robust Hotstart Ready Mix PCR kit (KapaBiosytems) and transgene specific primers: 5'-AGGCGATG ACAAAGAAGAG-3' and 3'-AGGGGATGAGGATGAAGAG-5'. Reaction conditions were: 1 cycle at 95°C for 2 min, 35 cycles as following: 94°C for 10 sec, 58°C for 10 sec and 72°C for 30 sec, and finally 1 cycle at 72°C for 7 min. PCR products were then separated on a 1 % agarose electrophoresis gel. Transgenic mice present a 470bp band while no band is detected in WT mice.

Mice sacrifice and eye removal

Most mice used in this study (140 mice) were sacrificed at PN 5 wk, according to previous studies showing that cell death is maximum between PN 5 and PN 6 wk. Procedures were performed in accordance with the animal use and care committee of the National Veterinary School of Alfort, France. Mice were sacrificed with CO_2 and eyes were immediately enucleated. Eyes were either directly mounted in Tissue-Tek O.C.T., frozen with liquid nitrogen and then cut in 10 µm frozen sections on a Leica CM3050 S freezing microtome. Alternatively, the eye was dissected, the retina removed and frozen at -20°C for protein studies.

Immunohistochemistry and TUNEL staining

Eye sections were washed in Ca^{2+}/Mg^{2+} supplemented PBS (phosphate-buffered saline, Life Technologies), incubated in 4% formaldehyde in PBS for 15 min for fixation, and washed with PBS. For permeabilization, they were incubated in 0.3% Triton X-100/PBS for 15 min and washed with PBS. Saturation was performed with 1 % nonfat milk in PBS for 1 hr. Sections were then incubated 1 hour with primary antibody in 0.1 % nonfat milk in

PBS. Antibodies used in this study are listed in **Table 1**. After washing the first antibody, samples were incubated with the second antibody in PBS for 1 hr in a dark chamber (used until the end of the staining). Nuclei were stained by 5 min incubation with DAPI (4-6 di-aminidino-2-henyl indoledichloride, Sigma) diluted 5000-fold in PBS. The tissue was mounted following the last wash: sections were cover slipped with fluoromount (Sigma). Negative controls with a non immune serum were run for each experiment. Due to the total negative result they were not incuded in the figures.

The TUNEL assay was performed according to the manufacturer's instructions (Roche Diagnostics, Mannheim, Germany), after the immunohistochemistry or just alone. In most of the cases, the TUNEL was preceded by a dephosphorylation step according to the protocol described by Lebon et al.(Lebon C et al., 2015). Briefly, sections were dephosphorylated with 10 U of calf intestinal alkaline phosphatase (CIAP, Invitrogen) in the associated buffer for 30 min at 37°C and washed. Images were acquired with a fluorescent U-25ND25 Olympus microscope. Image brightness and contrast were adjusted for display purposes when necessary with Image J software.

Western Blot

Retinas were defrosted on ice and homogenized in 100µl of M-Per buffer (Mammalian Protein Extraction Reagent, Thermo Scientific) supplemented with protease inhibitor cocktail (Roche Diagnostics) and incubated on ice for 15 min. Samples were then centrifuged at 8000 rpm for 3 min at 4°C. Supernatant was collected for protein measurement with the Pierce BCA Protein assay kit (Thermo Scientific). Laemmli sample buffer was added to the extracted material. Proteins were separated in a 12% SDS-PAGE and transferred on a nitrocellulose membrane (Whatman, GE Healthcare). Saturation was performed with 5% non-fat milk in PBS for 1 hr. The membrane was then incubated with primary antibody for 1 hr. at room temperature, washed with 0.1% tween in PBS, and incubated for 1 hr. with the secondary peroxidase labeled antibody. Antibodies used in this study are listed in **Table1**. After final washes with PBS, Luminata Forte Western HRP substrate (Millipore) was used to reveal the signal with the Microchemi 4.2 (DNR Bio-Imaging Systems). Image analysis and quantification was performed with ImageJ .

Intravitreous injections

Intravitrous injections were performed on PN 3 and 4 wk animals. Mice were anesthetized with Pentobarbital (Ceva) 50mg per kg via intraperitoneal injections and a drop of Tetracaïne (Novartis Pharma) was instilled on every eye. 1µl of solution was injected in the vitreous with the Micro4 micro-injector (World Precision Instruments).
siCtrl (Santa Cruz),siLEI (CCAUAAAUGUCCUCACUAU, Eurofins) and siAIF (GGAU CCUGACAUGCCAGACA, Eurofins) was diluted at 25 µM and 1 µl of this solution was incubated 5 min in 11 µl of TransIT buffer (Mirius) prior the injection. Calpain Inhibitor VI (Calbiochem) was diluted in PBS at concentration 600 nM and Pepstatin A (Sigma) was diluted at 40 µM. The control solution consisted of DMSO (Sigma) diluted 1/130 in PBS.

HEK293 cells

2 lines of stably transfected Human Embryonic Kidney 293 (HEK293) cells have been used in this study, kindly provided by Dr. YvonTrottier. Each line express either the wild-type human ataxin 7 protein (293-7N) or the mutant protein containing a polyQ expansion (293-7E), both containing a HA tag. Transgene expression is under doxycycline inducible promoter. Cells were cultured in Dulbecco's DMEM (4,5% glucose) supplemented with 5% Tet-system Approved FBS, 100U/ml penicillin streptomycin, 100µg/ml G418 and 25µg/ml hygromycine). To induce transgene expression, the medium was supplemented with doxycycline (3 or 6 µg/ml) during 24 hours. For immunochemistry, cells were washed with PBS and mounted on slide with a Cytospin-4 (Thermo Scientific) for 5 min at 1000 rpm. Immunocytochemistry was then performed according the same protocol than for immunohistochemistry as described above.

Statistical analysis

Statistics were performed using the GraphPad softweare (Prism). Due to the low number of samples non parametric tests were used. Results are shown as a median with an interquartile range. The specific test used in each experiment and the number of samples are indicated in each experiment.

Results

Ataxin7 expression induces stress in SCA7 mice retina

Previous studies reported that ataxin 790Q aggregates were detectable around and also within the nucleus in SCA7 R7E mice at PN 10 wk.(Helmlinger D,Abou-Sleymane G,Yvert G,Rousseau S,Weber C,Trottier Y,Mandel J-L and Devys D, 2004). At the same age, transgenic mice expressing human ataxin-7 with a 10Q tract presented a cytoplasmic localization of ataxin-7-10Q. At PN 5 wk., we could detect polyQ-ataxin7 expression in rods photoreceptors (**Fig.1A**). The expanded protein was found in the cytoplasm (in the outer and inner rods segment and around the nuclei) but also in the nuclei in some rods. Some polyQ accumulation was visible at this stage. Moreover, degradation of the polyQ protein was observed when studied by western blot (**Fig.1B**). The specific polyQ antibody allowed the detection of small peptides (20 and 30 kDa) containing a polyQ expansion. A small amount of full sized ataxin7polyQ (approx. 110 kDa) was detected on this blot. In addition, as early as in 5 weeks old mice, rods presented a significant reduction of rhodopsin expression in outer segments (**Fig.1C and D**). Interestingly, some rhodopsin positive cells were no longer in the photoreceptor layer but in the outer and inner plexiform layer. This was not observed in WT retina.Protein quantifications from western blot analysis showed the same results, with a significantly decrease of rhodopsin expression, mostly in its monomers and trimmers forms (**Fig.1D**).

In order to study the retinal stress induced by the toxicity of ataxin7 polyQ expression, we used Glial Fribrillary Acidic Protein (GFAP) as a marker of glial Müller cells activation. This intermediate filament is produced along the cell body of Müller cells during their gliosis in response to a non-specific stress. GFAP expression is increased in PN 5 wk.transgenic mice (**Fig. 2A and B**) compared to their WT littermate, indicating that Müller cells were activated.

Several studies have shown that polyQ toxicity due to the expression of expanded Huntingtin induced dysfunctional ERAD (Endoplasmic Reticulum Associated Degradation) process (Duennwald ML and Lindquist S, 2008) and UPR activation (Leitman J et al.,

2013). Three main pathways compose the UPR: PERK(PKR-like Endoplasmic Reticulum kinase), ATF-6 (Activating Transcription Factor 6) and IRE-1 (Inositol-requiring enzyme).We looked for UPR activation in our SCA7 mice through PERK expression. PERK expression was increased in photoreceptor cytoplasm (inner and outer photoreceptor segment layer) in 5 wk. SCA7 mice retinas compared to their WT littermate (**Fig. 3A**). However, we did not observe any increase in CHOP (C/EBP Homologous Protein) expression, a downstream marker of PERK pathway activation (not shown). Activation of IRE-1 pathway leads to an alternative splicing of XBP-1 (X-box binding protein 1) transforming it into a transcriptional factor that will modulate UPR genes expression. In SCA7 retina, we detected a small increase in XBP-1 unspliced form in both immunohistochemistry **(Fig. 3B)** and western blot analyzes (not shown). However, no spliced form was detected on the western blot of SCA7 retina. Interestingly, a higher expression of XBP-1 protein was also observed in HEK-293-7E cells and in HEK-293-7N cells (**not shown**). Recent studies have suggested a link between XBP-1 and autophagy via an increase of Forkhead box O1 (FoxO1) expression, a transcription factor regulating autophagy in neurons(16). We studied the expression of the p62 protein (also known as sequestosome 1) because it plays a role in the clearance of protein aggregates (Pankiv S et al., 2007) and has been described at the intersection between autophagy and apoptosis (Moscat J and Diaz-Meco MT, 2009). Immunohistochemistry reveals a dotted staining of this protein in ROS of SCA7 retina, which is not present in WT littermate (**Fig. 3C**). This specific staining suggests an accumulation of p62 in the cytoplasm and probably a decrease of the autophagic flux in SCA7 rods. However, no change in the expression level of p62 has been detected by western blot analysis (data not shown).

Taken together, these results suggest that the expression of the abnormal ataxin 7 produces retinal stress and a decrease of rhodopsin expression. The reticulum stress might be involved in this response.

SCA7 photoreceptors death did not involve the caspase pathway

It has been previously reported that SCA7 R7E mice retina displayed some photoreceptor death, most likely occurring between 5 and 6 weeks (Yefimova MG,Messaddeq N,Karam A,Jacquard C,Weber C,Jonet L,Wolfrum U,Jeanny J-C and Trottier Y, 2010). The use of the TUNEL (terminal deoxyribonucleotidyltransferase mediated dUTP-biotin nick end labeling) assay in order to detect dying rod nuclei did not allow the labeling of dying cells (**Fig.4A**). However, cell death could be detected with a modified TUNEL protocol that included a prior dephosphorylation step (Lebon C,Rodriguez GV,El Zaoui I,Jaadane I,Behar-Cohen F and Torriglia A, 2015). In the retina of SCA7 mice, dying nuclei were all localized in the outer nuclei layer, suggesting that only photoreceptors were dying. No cell death was detected in the retina of WT mice with this protocol (**Fig.4B**). Moreover, most cells ding are rod since the numberer of cones did not significantly change (not shown). The modification of the cell death detection protocol could indicate the type of cell death involved in this retinal degeneration. In the case of caspase-dependent cell death, DNA degradation by Caspase Activated DNase (CAD) is systematically detected with the classical TUNEL technique. The need for a dephosphorylation step might reflect the activation of a DNase II-type endonuclease in this process. However, to further investigate if caspases were involved in this cell death,we investigated the cleavage of caspase-3 and the cleavage of ACINUS (apoptotic chromatin condensation inducer in the nucleus).In caspase-dependent cell death, ACINUS is cleaved by active caspase-3 in a 23 kDa fragment that mediate apoptotic chromatin condensation previous to DNA fragmentation (Sahara S et al., 1999).Neither immunolabelling nor western blot analysis showed caspase-3 or ACINUS activation in SCA7 retinas compared to WT. Caspase-3 was only detected in the inner and outer photoreceptors segments in the retinas of WT and SCA7 mice (**Fig.5A**). No cleaved ACINUS was observed in photoreceptor nuclei of control or SCA7 mice. ACINUS staining was observed only in the inner nucleus layer in both control and transgenic mice (**Fig.5C**). In addition, western blot analysis did not present any cleaved form of caspase-3 or ACINUS, indicating that caspases were not involved in SCA7 rod death (**Fig.5B**). Taken together, these data suggest that the photoreceptor death observed in the retinas of SCA7 mice did not involve caspase-dependent cell death.

SCA7 photoreceptors death involved caspase-independent pathways

To further investigate this cell death we focused on two proteins AIF and LEI/L-DNase II. These cell death effectors were shown to be involved in caspase-independent cell death pathways. AIFplays an important role in mitochondrial respiration; it can be cleaved and delocalized into the nucleus upon apoptotic stimulus (Susin SA et al., 1999). LEI belongs to the Serpin family and its native form (42 kDa) has an anti-protease activity (Torriglia A and Lepretre C, 2009). After proteolytic cleavage, it becomes an endonuclease, L-DNase II (35 and 27 kDa), which is imported into the nucleus where it degrades DNA. It was shown, moreover, that these effectors might collaborate to facilitate DNA degradation during apoptosis (Leprêtre C et al., 2013). Immunostaining of these proteins combined with our adapted TUNEL staining allowed us to observe apoptotic photoreceptor nuclei in which there was a relocalization of both AIF and L-DNase II in the outer nuclear layer (**Fig.6A).** No nuclear staining was observed in the retinas of WT mice. Moreover, a laser microdissection of photoreceptor nuclei followed by a slot blot analysis showed an increase of LEI-L/DNase II and AIF in SCA7 photoreceptors nuclei compared to WT, for the same dissected surface (**Fig. 6B**). A western blot of WT and SCA7 retina and its quantification demonstrated significant increase of cleaved AIF (57 kDa) and of both forms of L-DNase II in SCA7 retina (**Fig.6C, D and E**). These results suggested the involvement of both AIF and LEI/L-DNase in SCA7 mice retinal degeneration. A cellular model for Sca7 has also been used to determine if LEI and AIF pathways activation depends on ataxin-7 polyQ expression. HEK-293 cells expressing either a 10Q ataxin7 (HEK-7N) or a 60Q ataxin7 (HEK-7E) were used. Exogene ataxin7 expression in those cells did not induced caspase-3 activation (data not shown). In case of expanded-ataxin7, its expression led to LEI-L/DNase II nuclear relocalization (**Fig. 7**) while no activation is observed when normal ataxin7 is expressed. Concerning AIF, its expression is increased in HEK-293-7E compared to HEK-293-7N but very few nuclear AIF was detected, suggesting that its release from mitochondria and its nuclearisation did not massively occur or occured after L-DNase II activation in this cellular model.

Inhibition of AIF and LEI expression lead to a decrease of photoreceptors death.

In order to validate these observations, we chose to inhibit AIF and LEI/L-DNase II expression in mice to see if retinal degeneration is affected. siRNA were injected intravitreously twice to 3- and 4 week-old mice and retinas were analyzed at 5 weeks as before. Dying cells were counted after injection using our adapted TUNEL staining. Quantification of both LEI and AIF expression after siLEI and siAIF injections, respectively, were performed on western blot analysis (**Fig. 8 and 9**). siLEI injection led to a decrease of LEI expression only in SCA7mice (**Fig. 8A and B**). A significant reduction of dying photoreceptor nuclei was observed in these mice (**Fig. 8C**). Intravitreous injection of siAIF induced a significant decrease of AIF expression in both WT and SCA7 retinas Fig 9A and B) and an important reduction of TUNEL positive cells was detected in SCA7 mice (**Fig.9 C**). It is important to note that inhibition of either AIF or LEI expression did not affect WT mice retina. The counting of photoreceptors death after siCtrl injection also permitted to evaluate cell death in SCA7 retinas compared to WT littermates where almost no dying photoreceptors were observed.Moreover, evaluation of the number of nuclei remaining in the ONL (**Fig. 9D**) indicates a stabilization of this layer upon siRNA treatment. Taken together these results tendedto confirm the implication of AIF and LEI in SCA7 photoreceptors cell death.

Calpains but not cathepsins seem to be related to AIF and LEI/L-DNase II activation

AIF released from mitochondria during cell death can be controlled by several factors. Among them calpains can directly cleave AIF and cathepsins are involved in AIF release through Bax activation (Delavallée L et al., 2011;Norberg E et al., 2010). On the other hand, LEI can be cleaved into L-DNase II by cathepsin D (Torriglia A and Lepretre C, 2009). In order to determine whether calpains or cathepsins were involved in AIF and L-DNase II activation in our model, we decided to inhibit each protease activity with intravitreous injections of their specific inhibitors. We used calpain inhibitor VI to inhibit calpains (both micro and mini calpains also called calpains 1 and 2) activities and pepstatin A to inhibit cathepsin D activity. The same protocol used for siRNA injection was applied and photoreceptor death was evaluated in the same way (**Fig. 10**). Calpain inhibitor VI

injections in SCA7 mice induced a significant reduction of cell death (**Fig. 10A**). However, pepstatinA injection did not show any significant effect (**Fig. 10B**). Neither pepstatin A nor calpain inhibitor VI induced toxicity in WT mice retina.

Discussion

In this study we analyzed the mechanisms of photoreceptors cell death due to polyQ toxicity induced by expanded ataxin7 expression in mice retina. We showed that two caspase-independent pathways mediate this cell death: LEI/L-DNase II and AIF.

Previous studies on SCA7 R7E mice demonstrated that this is a relevant model to study SCA7 human retinal degeneration since it reproduces what is seen in human pathology. SCA7 mice retinal degeneration is characterized by a very slow reduction of photoreceptors and intermediate cells layers. Outer and inner photoreceptor segments are first and soon disrupted while the amount of photoreceptors nuclei remains almost constant. However, Yefimov a*et al*, showed a peak of cell death between PN 5 and 6 wk (Yefimova MG,Messaddeq N,Karam A,Jacquard C,Weber C,Jonet L,Wolfrum U,Jeanny J-C and Trottier Y, 2010). The morphology of dying cells reminds apoptosis but no extensive study on the mechanisms involved in this cell death were performed. We chose to use PN 5 wk. mice to extend the possibility to observe and investigate dying photoreceptors, as it is a rare event.

Our first observation was that no apoptotic cells were detected with the TUNEL technique, widely used to detect dying cells. With an adjustment of the TUNEL protocol (by adding a dephosphorylation step prior the staining), we succeed in detecting apoptotic photoreceptor nuclei. At the same time, we observed a significant reduction in rhodopsin staining, which is consistent with previous studies and with the disappearance of outer and inner photoreceptor segments prior to nuclear layer reduction. This is an important result because it indicates that the DNase activity involved in this cell death exposes 3’P ends. The changes in the photoreceptors layer are accompanied by a deformation of this entire layer, forming "waves" along the retina. There is also an increase of GFAP staining, which suggests Müller cell activation. Those observations (rods loss, GFAP increase) have also been observed in model mice for human retinitis pigmentosa: the *rd/rd*mouse (Strettoi E et al., 2002). However, in this retinal degeneration, the cell layer reduction is quicker than in

the SCA7 mice. It is also important to note that rod loss happens while the polyQ ataxin-7 does not form detectable aggregates. According to Yvert et al., who set up the SCA7 R7E mice, aggregation (or nuclear inclusions) starts around PN 8 wk (Yvert G,Lindenberg KS,Picaud S,Landwehrmeyer GB,Sahel JA and Mandel J-L, 2000). We can therefore assume that soluble polyQ-ataxin-7 expression induces rods segment loss, as well as rod death and Müller cell activation.

We further studied the mechanisms involved in this cell death by first looking at the caspase pathway, although failing to label dying cells by regular TUNEL suggested a non-CAD (Caspaseactivated DNase) dependent cell death. As expected, neither caspase-3 nor ACINUS activation have been detected in the retina of SCA7 mice. Actually, no caspase-3 expression has been detected in the retinas of 5 wk old SCA7 and WT mice, which is consistent with previous studies on C57/bl6 retinal development showing that Apaf-1 and caspase-3 expression are strongly repressed in adult retina (Donovan M and Cotter T, 2002). In addition, light-induced retinal degeneration in mice has been shown to be caspase-3 independent as well as cell death in *rd* mouse photoreceptors (Arango-Gonzalez B et al., 2014;Donovan M et al., 2001). Taken together, these results suggest that photoreceptor cell death does not depend on caspase pathways and might involve a caspase-independent mechanism. Indeed, the need of a dephosphorylation step to detect DNA degradation informs us on the type of DNA breaks. 3'OH breaks are recognized by the terminal tranferase in the TUNEL assay, while 3'P ends are not, leading to a TUNEL negative labeling. However, after a dephosphorylation step, 3'P ends become 3'OH and are now recognized by the TUNEL enzyme. This particularity has been described previously by our team and others (Lebon C,Rodriguez GV,El Zaoui I,Jaadane I,Behar-Cohen F and Torriglia A, 2015) (Hayashi R et al., 1998), specifically the in case of LEI/L-DNase II activation which is a 3’P producing endonuclease. This protein was described by Torriglia et al. in 1995 during lens cell differentiation (Torriglia A et al., 1995;Torriglia A et al., 1998) (Padron-Barthe L et al., 2007) and has been involved in different rats retinal paradigms: glucocorticoids-induced retinal toxicity or different types of light-induced retinal degeneration (Chahory S et al., 2004;El Zaoui I et al., 2014;Jaadane I et al., 2015). It has also been demonstrated that LEI/L-DNase II can collaborate with AIF, another caspase-independent pathway, to induce cell death in vitro (Leprêtre C,Tchakarska G,Blibech H,Lebon C and Torriglia A, 2013). AIF nuclear translocation was described in an induced

retinal detachment rat model and in a LED-induced retinal degeneration in rats (Jaadane I,Boulenguez P,Chahory S,Carré S,Savoldelli M,Jonet L,Behar-Cohen F,Martinsons C and Torriglia A, 2015). So that, we have investigated these two cell death effectors and shown here that both are translocated to the nucleus of TUNEL positive photoreceptors. In addition, LEI/L-DNase II is also translocated to the nucleus after expanded ataxin7 expression in our in vitro cellular model in a more systematic way than AIF. This observation is consistent with previous results showing that L-DNase II precedes AIF into the nucleus and with the hypothesis that L-DNase II might, in some cases, contribute to the nuclear translocation of AIF via the activation of PARP and the release of PAR (Leprêtre C,Tchakarska G,Blibech H,Lebon C and Torriglia A, 2013). AIF and LEI/L-DNase II activation in SCA7 photoreceptors death have been confirmed by intravitreous injections of specific siRNA. When either LEI or AIF are downregulated, the number of apoptotic photoreceptors is significantly decreased. However, there are still dying photoreceptors after two siRNA injections suggesting that either inhibition was not enough efficient or others pathways could be involved. It might be interesting to inhibit both AIF and LEI in the same time to see if there is a cumulative effect on cell death receptors. However, this is a difficult task because both LEI and AIF have anti-apoptotic functions in their cytoplasmic/ mitochondrial forms (Daugas E et al., 2000;Padron-Barthe L,Lepretre C,Martin E,Counis MF and Torriglia A, 2007).

In order to explore the activation mechanism of those two caspase-independent cell death effectors, we chose to inhibit calpain activation pathway with calpain inhibitor VI and cathepsin D pathway with Pepstatin A injection, both inhibitors already used in previous studies (Chahory S et al., 2010;Rodriguez GEV and Torriglia A, 2013). Our results suggest that AIF and LEI activation depends, at least in part of calpain 1 (or micro-calpain). Indeed, calpain 1 is the protease responsible for the release of AIF from mitochondria and it plays also a role in lysosomal permeabilisation, leading to the release of cathepsin D from the lysosome among others lysosomal proteins (Chen Q and Lesnefsky EJ, 2015;Rodriguez GEV and Torriglia A, 2013). As cathepsin D is also responsible for LEI cleavage into L-DNase II, calpain 1 inhibition activity may prevent both cell death effectors activation. It is the case in this SCA7 degeneration since injection of calpain inhibitor VI (at a dose that specifically inhibits calpain 1 activity) (Rodriguez GEV and Torriglia A, 2013) , produced a decrease in the number of dying cells. Calpain1 inhibition has also been used to reduce

cardiac cell death in a myocardial infarction model (Smith MA and Schnellmann RG, 2012). Concerning cathepsin D activity inhibition by pepstatine A, no significant effect on photoreceptors cell death has been observed, suggesting that LEI cleavage into L-DNase II involves other proteases such elastase which is its specific substrate, AP24 (Apoptotic Protease 24 kDa) or other serine proteases (O'connell A et al., 2006). These results differ from what has been observed in light-induced retinal degeneration in rats in which pepstatin A injection prevented photoreceptors death due to LEI activation (Chahory S,Keller N,Martin E,Omri B,Crisanti P and Torriglia A, 2010). Another possibility could be that, when LEI cleavage is inhibited by pepstatin A, AIF is still released from mitochondria and relocated into the nucleus where it can mediates DNA degradation through endonuclease G (endo G) activation. Indeed, endo G is also a type II nuclease, originally located in the mitochondria and involved in mitochondrial replication (Li LY et al., 2001). It can be released from the mitochondria in a caspase-independent manner, such as AIF, and translocate into the nucleus where it degrades DNA (van Loo G et al., 2001). Endo G has been involved in neuronal cell death due to glutamate excitotoxity in mice hippocampus (Wu Y et al., 2004).

It has been previously reported that polyQ proteins induce endoplasmic reticulum stress accompanied by an unfolded protein response. Studies, mostly concerning huntingtin, the protein responsible for Huntington's disease, demonstrated that the three branches of UPR are involved in the response to polyQ toxicity and ERAD inhibition (Jiang Y et al., 2016;Ogen-Shtern N et al., 2016). This phenomenon is shared by other misfolding protein diseases such Alzheimer's or Parkinson's (Leitman J,Hartl FU and Lederkremer GZ, 2013). Our 5 wk. SCA7 mice rods do not present ataxin7 aggregates but nuclear inclusions are detected at 10 wk. (Helmlinger D,Abou-Sleymane G,Yvert G,Rousseau S,Weber C,Trottier Y,Mandel J-L and Devys D, 2004). Here we show that some branches of the UPR are already activated at 5 wk. such as the PERK pathway. XBP-1 expression is increased but no spliced form has been detected. However, CHOP up-regulation has not been observed. When ERAD and UPS (Ubiquitin Proteasome System) are not sufficient to manage misfolded protein, autophagy can be activated. In our model, p62 bodies are detected suggesting that p62 binds to autophagosomes to clear misfolded proteins and aggregates. However, it also suggests an impairment in the autophagy machinery since p62 accumulates in ROS (Giansanti V et al., 2011). If all the systems involved in protein

clearance are deficient or overwhelmed by the expression of polyQ proteins, cells activate apoptotic pathways. The mechanisms involved in the switch between autophagy and caspase-independent apoptosis remain to be elucidated.

Studies on polyQ diseases are mainly focused on Huntington's disease and concern brain or in vitro models. SCA7 is the only polyQ disease affecting the retina and deciphering the toxicity and cell death mechanisms induced by abnormal ataxin 7 in retina may contribute to the advancement of knowledge on neuro-proteinopathies.

Acknowledgments: We are grateful to Julia Pardo and Laurent Jonet for technical assistance and to Cathy Claramonte and Dr. Sabine Chahory for their assistance in the animal care. We are thankful to Alejandro Arboleda for his English editing. This work was supported by INSERM and Cecile Lebon had a fellowship from Paris Descartes University and from the CRO association. CL made the experiments and wrote de paper, FBC gave scientific advice, AT conducted the work designed the experiments and wrote the paper.

Bibliography

Arango-Gonzalez B, Trifunović D, Sahaboglu A, Kranz K, Michalakis S, Farinelli P, Koch S, Koch F, et al. (2014), Identification of a common non-apoptotic cell death mechanism in hereditary retinal degeneration. PloS one 9:e112142.

Chahory S, Keller N, Martin E, Omri B, Crisanti P, Torriglia A (2010), Light induced retinal degeneration activates a caspase-independent pathway involving cathepsin D. Neurochem Int 57:278-287.

Chahory S, Padron L, Courtois Y, Torriglia A (2004), The LEI/L-DNase II pathway is activated in light-induced retinal degeneration in rats. Neuroscience letters 367:205-209.

Chen Q, Lesnefsky EJ (2015), Heart mitochondria and calpain 1: location, function, and targets. Biochimica et Biophysica Acta (BBA)-Molecular Basis of Disease 1852:2372-2378.

Daugas E, Nochy D, Ravagnan L, Loeffler M, Susin SA, Zamzami N, Kroemer G (2000), Apoptosis-inducing factor (AIF): a ubiquitous mitochondrial oxidoreductase involved in apoptosis. FEBS letters 476:118-123.

David G, Abbas N, Stevanin G, Dürr A, Yvert G, Cancel G, Weber C, Imbert G, et al. (1997), Cloning of the SCA7 gene reveals a highly unstable CAG repeat expansion. Nature genetics 17:65.

Delavallée L, Cabon L, Galán-Malo P, Lorenzo HK, Susin SA (2011), AIF-mediated caspase-independent necroptosis: A new chance for targeted therapeutics. IUBMB life 63:221-232.

Donovan M, Carmody RJ, Cotter TG (2001), Light-induced photoreceptor apoptosis in vivo requires neuronal nitric-oxide synthase and guanylate cyclase activity and is caspase-3-independent. Journal of biological chemistry 276:23000-23008.

Donovan M, Cotter T (2002), Caspase-independent photoreceptor apoptosis in vivo and differential expression of apoptotic protease activating factor-1 and caspase-3 during retinal development. Cell death and differentiation 9:1220.

Duennwald ML, Lindquist S (2008), Impaired ERAD and ER stress are early and specific events in polyglutamine toxicity. Genes & development 22:3308-3319.

El Zaoui I, Behar-Cohen F, Torriglia A (2014), Glucocorticoids exert direct toxicity on microvasculature: analysis of cell death mechanisms. Toxicological Sciences 143:441-453.

Garden GA, La Spada AR (2008), Molecular pathogenesis and cellular pathology of spinocerebellar ataxia type 7 neurodegeneration. The Cerebellum 7:138-149.

Giansanti V, Torriglia A, Scovassi AI (2011), Conversation between apoptosis and autophagy:“Is it your turn or mine?”. Apoptosis 16:321-333.

Hayashi R, Ito Y, Matsumoto K, Fujino Y, Otsuki Y (1998), Quantitative differentiation of both free 3'-OH and 5'-OH DNA ends between heat-induced apoptosis and necrosis. J Histochem Cytochem 46:1051-1059.

Helmlinger D, Abou-Sleymane G, Yvert G, Rousseau S, Weber C, Trottier Y, Mandel J-L, Devys D (2004), Disease progression despite early loss of polyglutamine protein expression in SCA7 mouse model. Journal of Neuroscience 24:1881-1887.

Jaadane I, Boulenguez P, Chahory S, Carré S, Savoldelli M, Jonet L, Behar-Cohen F, Martinsons C, et al. (2015), Retinal damage induced by commercial light emitting diodes (LEDs). Free radical biology and medicine 84:373-384.

Jiang Y, Chadwick SR, Lajoie P (2016), Endoplasmic reticulum stress: The cause and solution to Huntington's disease? Brain research 1648:650-657.
Lebon C, Rodriguez GV, El Zaoui I, Jaadane I, Behar-Cohen F, Torriglia A (2015), On the use of an appropriate TdT-mediated dUTP–biotin nick end labeling assay to identify apoptotic cells. Analytical biochemistry 480:37-41.
Leitman J, Hartl FU, Lederkremer GZ (2013), Soluble forms of polyQ-expanded huntingtin rather than large aggregates cause endoplasmic reticulum stress. Nature communications 4:2753.
Leprêtre C, Tchakarska G, Blibech H, Lebon C, Torriglia A (2013), Apoptosis-inducing factor (AIF) and leukocyte elastase inhibitor/L-DNase II (LEI/LDNaseII), can interact to conduct caspase-independent cell death. Apoptosis 18:1048-1059.
Li LY, Luo X, Wang X (2001), Endonuclease G is an apoptotic DNase when released from mitochondria. Nature 412:95.
Michalik A, Martin J, Van Broeckhoven C (2004), Spinocerebellar ataxia type 7 associated with pigmentary retinal dystrophy. European journal of human genetics 12:2.
Moscat J, Diaz-Meco MT (2009), p62 at the crossroads of autophagy, apoptosis, and cancer. Cell 137:1001-1004.
Norberg E, Orrenius S, Zhivotovsky B (2010), Mitochondrial regulation of cell death: processing of apoptosis-inducing factor (AIF). Biochemical and biophysical research communications 396:95-100.
O'connell A, Holohan C, Torriglia A, Lee B, Stenson-Cox C (2006), Characterization of a serine protease-mediated cell death program activated in human leukemia cells. Experimental cell research 312:27-39.
Ogen-Shtern N, David TB, Lederkremer GZ (2016), Protein aggregation and ER stress. Brain research 1648:658-666.
Padron-Barthe L, Lepretre C, Martin E, Counis MF, Torriglia A (2007), Conformational modification of serpins transforms leukocyte elastase inhibitor into an endonuclease involved in apoptosis. Mol Cell Biol 27:4028-4036.
Pankiv S, Clausen TH, Lamark T, Brech A, Bruun J-A, Outzen H, Øvervatn A, Bjørkøy G, et al. (2007), p62/SQSTM1 binds directly to Atg8/LC3 to facilitate degradation of ubiquitinated protein aggregates by autophagy. Journal of biological chemistry 282:24131-24145.
Rodriguez GEV, Torriglia A (2013), Calpain 1 induce lysosomal permeabilization by cleavage of lysosomal associated membrane protein 2. Biochimica et Biophysica Acta (BBA)-Molecular Cell Research 1833:2244-2253.
Sahara S, Aoto M, Eguchi Y, Imamoto N, Yoneda Y, Tsujimoto Y (1999), Acinus is a caspase-3-activated protein required for apoptotic chromatin condensation. Nature 401:168.
Smith MA, Schnellmann RG (2012), Calpains, mitochondria, and apoptosis. Cardiovascular research 96:32-37.
Strettoi E, Porciatti V, Falsini B, Pignatelli V, Rossi C (2002), Morphological and functional abnormalities in the inner retina of the rd/rd mouse. Journal of Neuroscience 22:5492-5504.
Susin SA, Lorenzo HK, Zamzami N, Marzo I, Snow BE, Brothers GM, Mangion J, Jacotot E, et al. (1999), Molecular characterization of mitochondrial apoptosis-inducing factor. Nature 397:441-446.

Torriglia A, Chaudun E, Chany-Fournier F, Jeanny J-C, Courtois Y, Counis M-F (1995), Involvement of DNase II in nuclear degeneration during lens cell differentiation. Journal of biological chemistry 270:28579-28585.
Torriglia A, Lepretre C (2009), LEI/L-DNase II: interplay between caspase-dependent and independent pathways. Frontiers in bioscience (Landmark edition) 14:4836-4847.
Torriglia A, Perani P, Brossas JY, Chaudun E, Treton J, Courtois Y, Counis M-F (1998), L-DNase II, a molecule that links proteases and endonucleases in apoptosis, derives from the ubiquitous serpin leukocyte elastase inhibitor. Molecular and cellular biology 18:3612-3619.
van Loo G, Schotte P, Van Gurp M, Demol H, Hoorelbeke B, Gevaert K, Rodriguez I, Ruiz-Carrillo A, et al. (2001), Endonuclease G: a mitochondrial protein released in apoptosis and involved in caspase-independent DNA degradation. Cell death and differentiation 8:1136.
Wu Y, Dong M, Toepfer NJ, Fan Y, Xu M, Zhang J (2004), Role of endonuclease G in neuronal excitotoxicity in mice. Neuroscience letters 364:203-207.
Yefimova MG, Messaddeq N, Karam A, Jacquard C, Weber C, Jonet L, Wolfrum U, Jeanny J-C, et al. (2010), Polyglutamine toxicity induces rod photoreceptor division, morphological transformation or death in spinocerebellar ataxia 7 mouse retina. Neurobiology of disease 40:311-324.
Yvert G, Lindenberg KS, Picaud S, Landwehrmeyer GB, Sahel JA, Mandel J-L (2000), Expanded polyglutamines induce neurodegeneration and trans-neuronal alterations in cerebellum and retina of SCA7 transgenic mice. Human Molecular Genetics 9:2491-2506.

Captions to figures:

Figure 1: **Retinal degeneration induced by polyQ expression.** (A) polyQ (in red) staining in 5 wk. WT and SCA7 retinas. Black arrows show ONL enlargement. Nuclei are stained in blue with Dapi. (B) Western Blot analysis of WT and SCA7 retinas with anti-polyQ antibodies. Actin was used as a charge control. (C) Rhodopsin immunostaining (in green) of WT and SCA7 retinas. Nuclei are stained in blue with Dapi. ONL indicates the outer nuclear layer, INL the inner nuclear layer. Scale bar represents 30 μm.
(D) Representative western blot of rhodospin expression in WT and SCA7 retinas, and its densitometric analysis (quantification was normalized to actin level).T, D and M represent the different forms of rhodopsin namely trimers, dimers and monomers. Medians are represented by lines. Statistical calculations were performed using Mann Whitney test, $U(n3,n3)=0.0$, $p \leq 0.05$

.

Figure 2: Müller cells are activated in SCA7 retina. (A) anti-Glial Fibrillary Acid Protein antibody (in red) was used to observe Müller cells activation in WT and SCA7 retinas. Nuclei are stained in blue with Dapi. ONL indicates the outer nuclear layer, INL the inner nuclear layer. Scale bar represents 30 μm. (B) Western blot and its densitometric analysis of WT and SCA7 retinas with anti-GFAP antibodies. Actin and ponceau red were used as charge controls. Medians are represented by lines Statistical calculations were performed using Mann Whitney test $U(n3,n3)=0.0$, $p \leq 0.05$.

Figure 3: **The ER stress is activated in SCA7 retina.**(A) PERK immunostaining (in red) of 5 wk. WT and SCA7 retinas. (B**)** XBP-1 staining (in red) in WT and SCA7 5 wk. retinas.(C) p62 staining (in red) in SCA7 retina compared to WT littermate. Black arrows indicate enlargement of the outer nuclear and receptor layers. Nuclei are stained in blue with Dapi. ONL indicates the outer nuclear layer, INL the inner nuclear layer. Scale bar represents 30μm.

Figure 4: **Detection of photoreceptors death in SCA7 retina.** (A) No cell death (in green) is detected in WT and SCA7 retinas using classic TUNEL protocol. Dying photoreceptors are only detected with a dephosphorylation prior to the TUNEL assay in

SCA7 retina (SCA7+Ph). Scale bar represents 30 μm. ONL indicates the outer nuclear layer, INL the inner nuclear layer. (B) Detection of cell death (in green) in the whole retina using a modified TUNEL assay. White arrows indicate some TUNEL positive cells. Nuclei are stained in blue with Dapi. Cornea is on the left, optical nerve on the right. Scale bar represents 150μm.

Figure 5: **Caspase 3 and ACINUS are not activated in photoreceptors death.** (A) Staining of activated caspase3 (in green) in WT and SCA7 retinas. Nuclei are stained in blue with Dapi. (B) Western blot analysis of WT and SCA7 retinas with anti-activated-caspase3 and anti-ACINUS antibodies. Actin and red ponceau are used as a charge control. Etoposide-treated HeLa cells are used as a positive control for caspase3 activation and acinus cleavage.(C) Staining of ACINUS (in red) in WT and SCA7 retinas. Nuclei are stained in blue with Dapi. ONL indicates the outer nuclear layer, INL the inner nuclear layer. Scale bar represents 30μm.

Figure 6: **LEI/L-DNase II and AIF are activated in SCA7 retina.** (A) Co-staining of LEI/L-DNase II (in blue), AIF (in red) and modified TUNEL assay (in green). White arrows indicate TUNEL positive nuclei in which both LEI/L-DNase II and AIF are translocated in SCA7 retina. Nuclei are stained in blue with Dapi. ONL indicates the outer nuclear layer, INL the inner nuclear layer. Scale bar represents 30μm. (B) Quantification of the expression of LEI/L-DNase II and AIF in the ONL. The samples were obtained by laser microdissection of the ONL. The amount of the proteins present in this layer was quantified by dot blot,
Medians are represented by lines Statistical calculations were performed using Mann Whitney test. LEI: $U(n8,n8)= 2.0$, , $p \leq 0.005$. AIF: $U(n6,n6)= 3.0$, , $p \leq 0.05$
.
(C) Western blot analysis of WT and SCA7 retinas with anti-AIF and anti-LEI/L-DNase II antibodies (representative image). Actin and ponceau red were used as a charge control (D) A densitometric analysis of the represented western blot for AIF and activated AIF (AIFt) Statistical calculations were performed using Mann Whitney test. Medians are represented by lines Statistical calculations were performed using Mann Whitney test. AIF: $U(n4,n4)= 0.0$, , $p \leq 0.05$. tAIF: $U(n4,n4)= 0.0$, , $p \leq 0.05$

. (E) densitometric analysis for LEI and its two activated forms. Quantification was normalized to actin level. Medians are represented by lines. Statistical calculations were performed using Mann Whitney test. LEI: U(n4,n4)= 0.0, p = , $p \leq 0.05$. p35: U(n4,n4)= 11.0, p =, $p \leq 0.05$

Figure 7: AIF and LEI expression in HEK293 cells

HEK-293-7N and HEK-293-7E cells were co-stained for AIF (red)and LEI/L-DNase II (green).White arrows show nuclear localization of LEI/L-DNase II in cells expressing the expanded ataxin7. Nuclei are stained in blue with Dapi.Scale bar represents 10µM.

Figure 8: Inhibition of LEI expression reduces photoreceptors death in SCA7 retina.

(A) Quantification of LEI expression in WT and SCA7 retinas after intravitreous injections of siRNA Ctrl or LEI. Densitometric analysis of western blot has been normalized to actin level. . Statistical calculations were performed using Kruskal-Wallis and a Dunn's postest, H(4)= 13.76, $p<0.051$ (B) LEI immunostaining (in green) in SCA7 retina after siRNA Ctrl or LEI injections. Nuclei are stained in blue with Dapi. ONL indicates the outer nuclear layer, INL the inner nuclear layer. Scale bar represents 30µm. (C) Evaluation of TUNEL positive nuclei after siRNA injection in WT and SCA7 mice. Statistical calculations were performed using Kruskal-Wallis and a Dunn's postest, H(4)= 13.78, $p<0.05$

Figure 9: **Inhibition of AIF expression reduces photoreceptors death in SCA7 retina.**

(A) Quantification of AIF expression in WT and SCA7 retinas after intravitreous injections of siRNA Ctrl or AIF. Densitometric analysis of western blot has been normalized to actin level. Statistical calculations were performed using Kruskal-Wallis and a Dunn's postest, H(4)= 13.76 $p<0.05$ (B) AIF immunostaining (in green) in SCA7 retina after siRNA Ctrl or AIF injections. Nuclei are stained in blue with Dapi. ONL indicates the outer nuclear layer, INL the inner nuclear layer. Scale bar represents 30µm. (C) Evaluation of TUNEL positive nuclei after siRNA injection in WT and SCA7 mice. Statistical calculations were performed using Kruskal-Wallis and a Dunn's postest, H(4)= 17.58, $p<0.05$ (D) The density of the remaining nuclei in ONL was counted using DAPI coloration and a ImageJ calculation. WT and SCA7 controls were injected with the control SiRNA. Statistical calculations were performed using Kruskal-Wallis and a Dunn's postest, H(6)= 26.6, $p<0.05$

(B) Figure 10: **Effects of intravitreous injections of Calpain inhibitor VI and pepstatin A.A on cell death. (**A) Evaluation of photoreceptors death by the modified TUNEL assay after Calpain inhibitor VI injections in WT and SCA7 mice. Statistical calculations were performed using Kruskal-Wallis and a Dunn's postest, $H(4)= 13.45$, $p<0.05$ (B) Evaluation of photoreceptors death by the modified TUNEL assay after Pepstatin A injections in WT and SCA7 mice. Statistical calculations were performed using Kruskal-Wallis and a Dunn's postest, $H(4)= 13.45$ $p<0.1$

Table 1: Antibodies used in this study

Antibody name	**Supplier**	**Immunochemistry Dilution**	**Western Blot Dilution**
AIF	Abcam	1/100	-
AIF	Santa Cruz	-	1/1000
LEI-L/DNase II	(24)	1/100	1/1000
polyGlutamines (1C2)	Millipore	1/200	1/2000
GFAP	Dako	1/200	1/1000
Rhodopsine (Rho4D2)	Abcam	1/200	1/1000
cleavedCaspase 3	Cell signaling	1/100	1/500
Acinus	BioRad	1/200	1/1000
MAP lc3	Santa Cruz	1/100	-
β-actine-HRP	Santa Cruz	-	1/10000
actine	Santa Cruz	-	1/1000
Lamine B	Santa Cruz	-	1/1000
HSP 70	BD Biosciences	-	1/1000
p62	Sigma	1/100	1/1000
Cathepsin B	Calbiochem	1/200	-
PERK	Santa Cruz	1/100	-
pH2A.X	Millipore	1/100	-
Calpain I	BioVision	1/200	-
HA	Roche	1/200	1/5000
Ataxin7 N-ter& C-ter	Sigma	1/100	
Peroxydase labeled anti-goat	Vector	-	1/5000
Peroxydase labeled anti-mouse	Vector	-	1/5000
Peroxydase labeled anti-rabbit	Vector	-	1/5000

Alexafluor 546 anti-goat	Invitrogen	1/200	-
Alexafluor 546 anti-rabbit	Invitrogen	1/200	-
Alexafluor 594 anti-mouse	Invitrogen	1/200	-
Alexafluor 488 anti-mouse	Invitrogen	1/200	-
Alexafluor 488 anti-goat	Invitrogen	1/200	-
Alexafluor 488 anti-goat	Invitrogen	1/200	-
Pacific Blue anti-rabbit	Invitrogen	1/200	-

Table 1: Antibodies used in this study and their dilution according the technique

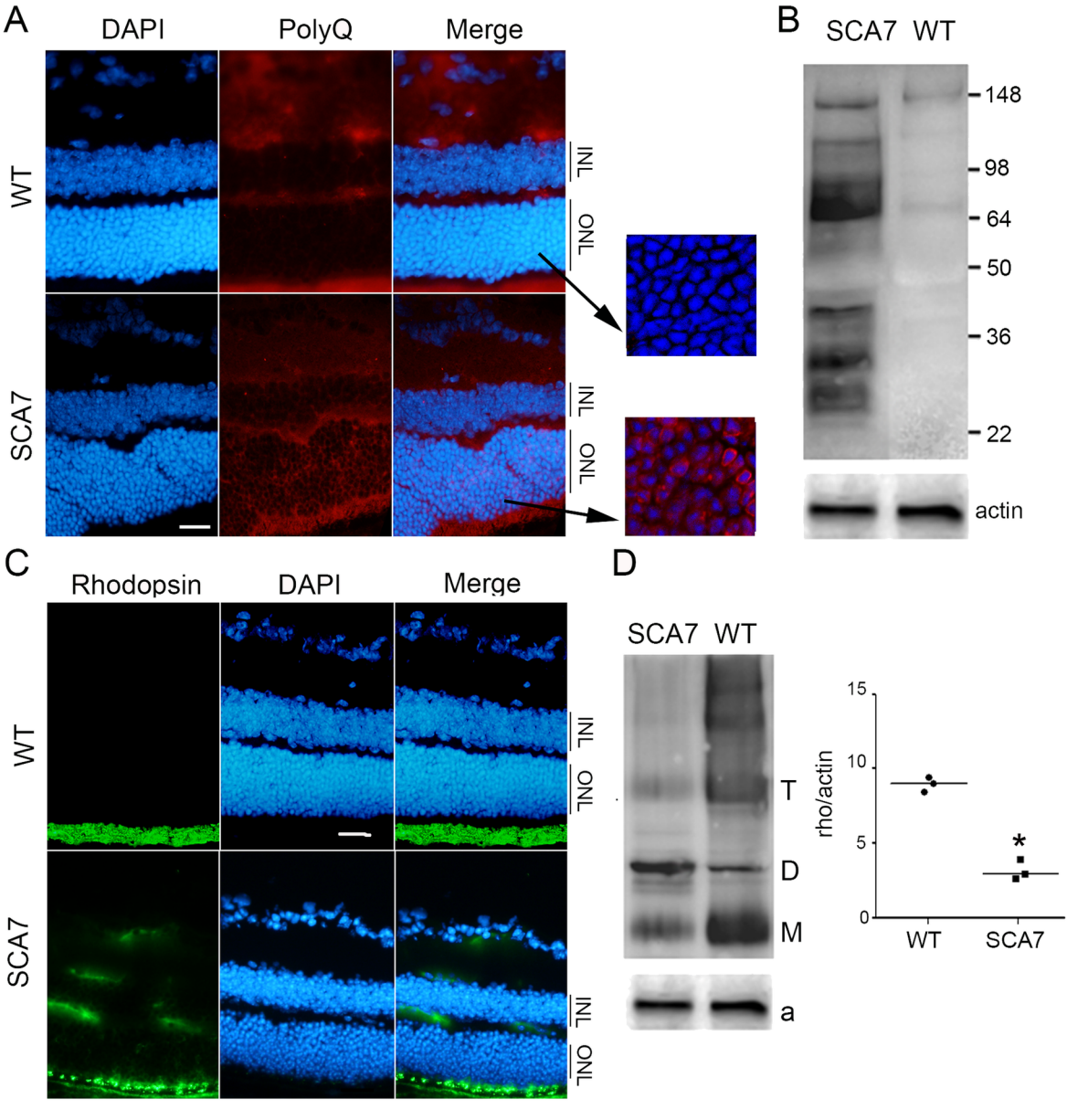
A
DAPI
PolyQ
Merge
WT
SCA7
INL
ONL
INL
ONL
B
SCA7 WT
148
98
64
50
36
22
actin
C
Rhodopsin
DAPI
Merge
WT
SCA7
INL
ONL
INL
ONL
D
SCA7 WT
T
D
M
a
rho/actin
15
10
5
0
*
WT
SCA7

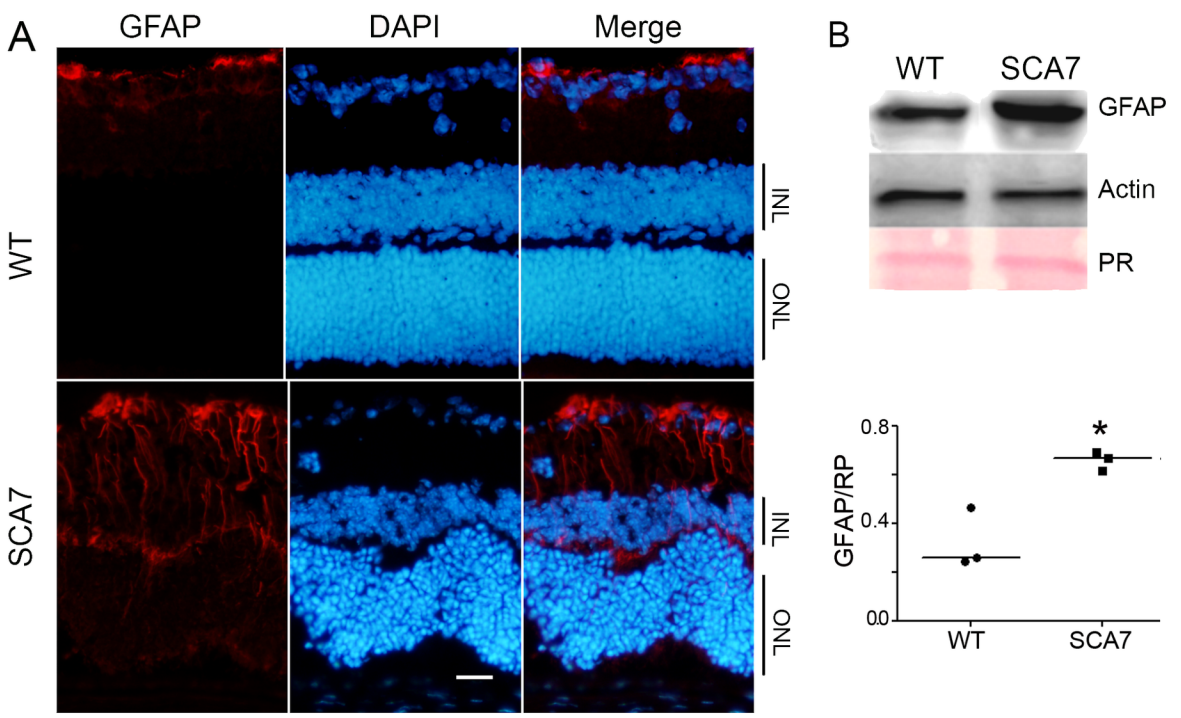
A
GFAP
DAPI
Merge
WT
SCA7
INL
ONL
INL
ONL
B
WT
SCA7
GFAP
Actin
PR
GFAP/RP
0.8
0.4
0.0
*
WT
SCA7

A
DAPI
PERK
Merge
WT
SCA7
INL
ONL
INL
ONL
B
DAPI
XBP-1
Merge
WT
SCA7
INL
ONL
INL
ONL
C
DAPI
p62
Merge
WT
SCA7
INL
ONL
INL
ONL

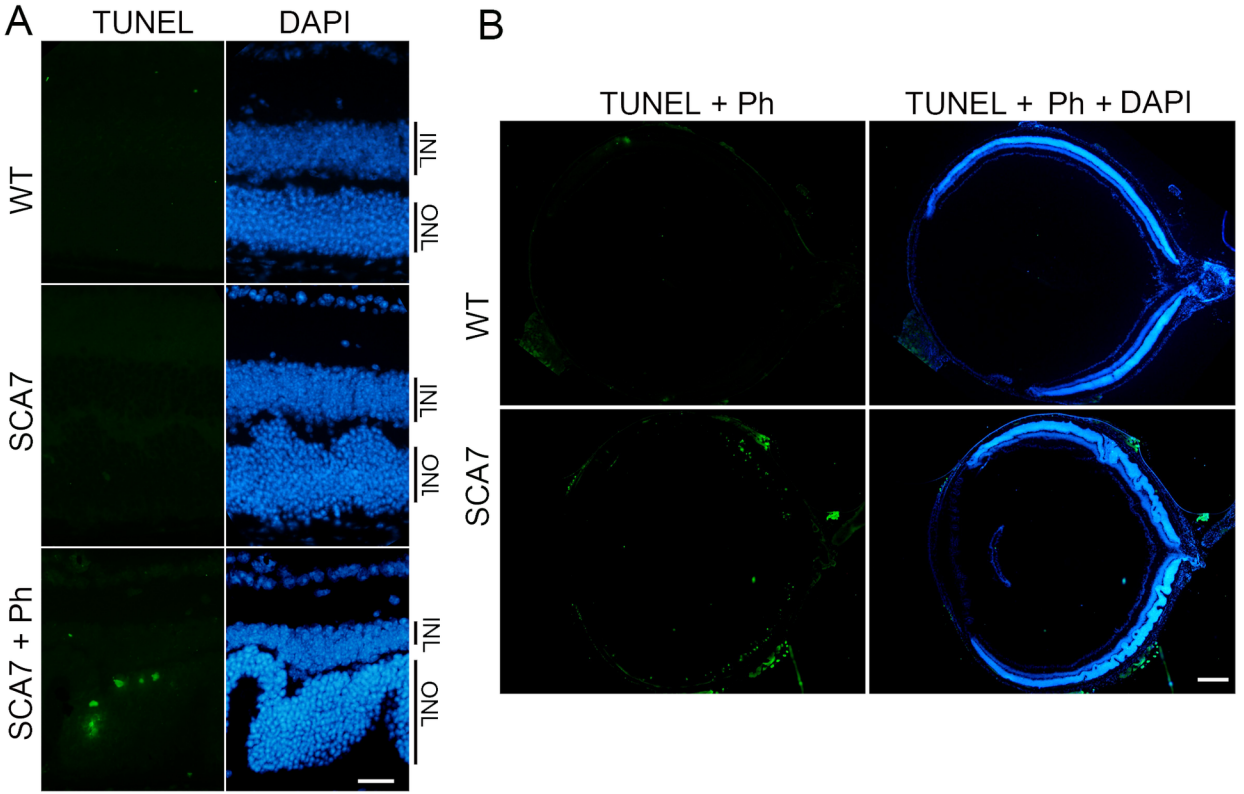
A
TUNEL
DAPI
WT
SCA7
SCA7 + Ph
INL
ONL
INL
ONL
INL
ONL
B
TUNEL + Ph
TUNEL + Ph + DAPI
WT
SCA7

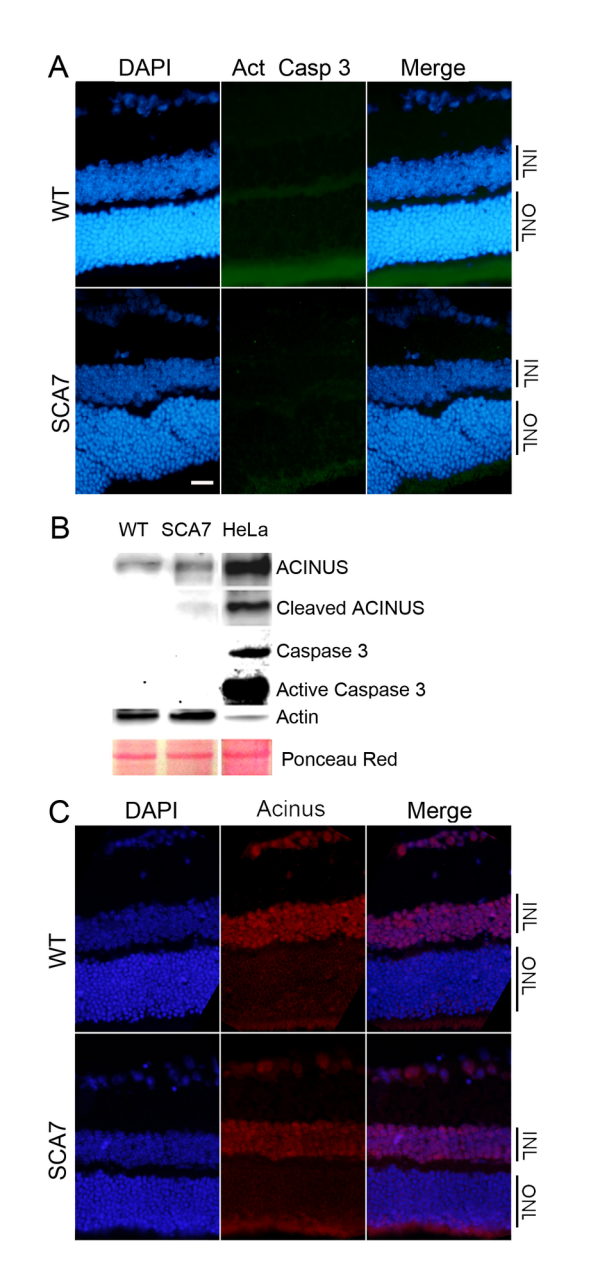
A
DAPI
Act Casp 3
Merge
WT
SCA7
INL
ONL
INL
ONL
B
WT SCA7 HeLa
ACINUS
Cleaved ACINUS
Caspase 3
Active Caspase 3
Actin
Ponceau Red
C
DAPI
Acinus
Merge
WT
SCA7
INL
ONL
INL
ONL

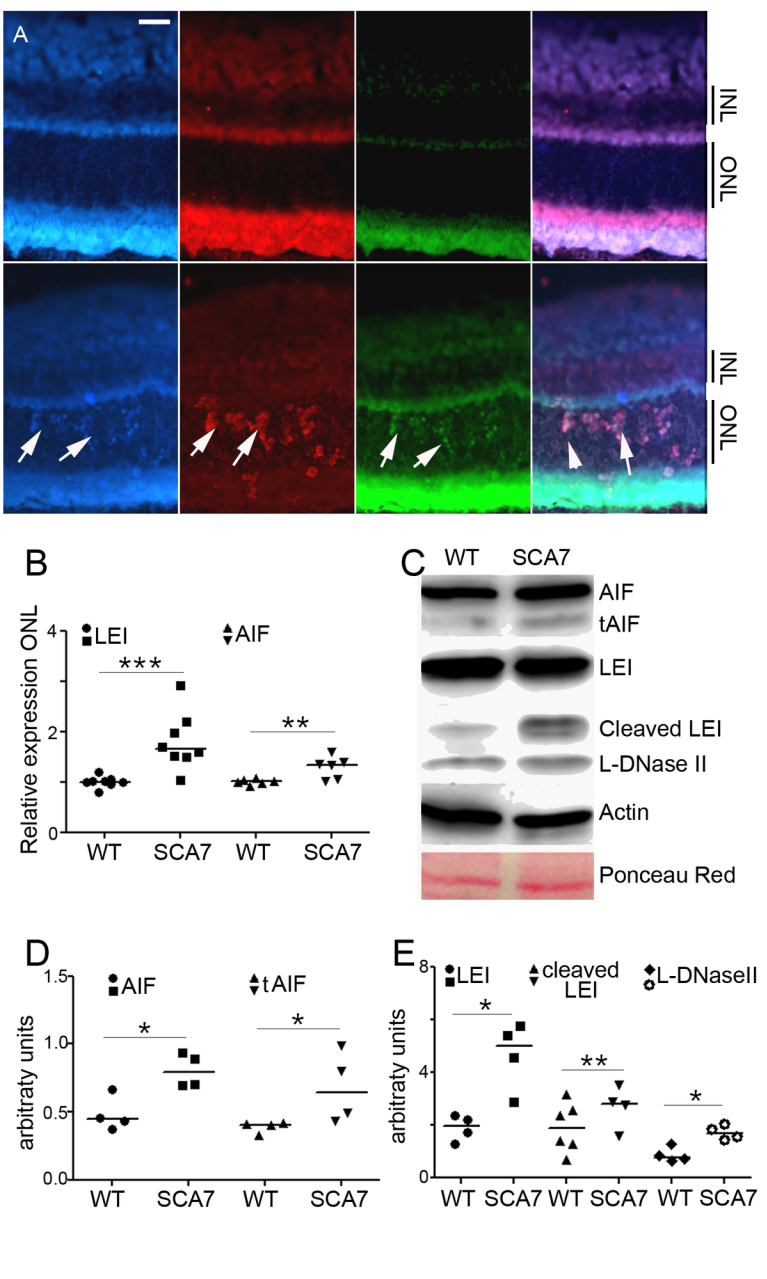
A
INL
ONL
INL
ONL
B
LEI
AIF
Relative expression ONL
4
2
0
***
**
WT
SCA7
WT
SCA7
C
WT
SCA7
AIF
tAIF
LEI
Cleaved LEI
L-DNase II
Actin
Ponceau Red
D
AIF
tAIF
arbitraty units
1.5
1.0
0.5
0.0
*
*
WT
SCA7
WT
SCA7
E
LEI
cleaved LEI
L-DNaseII
arbitraty units
8
4
0
*
**
*
WT
SCA7
WT
SCA7
WT
SCA7

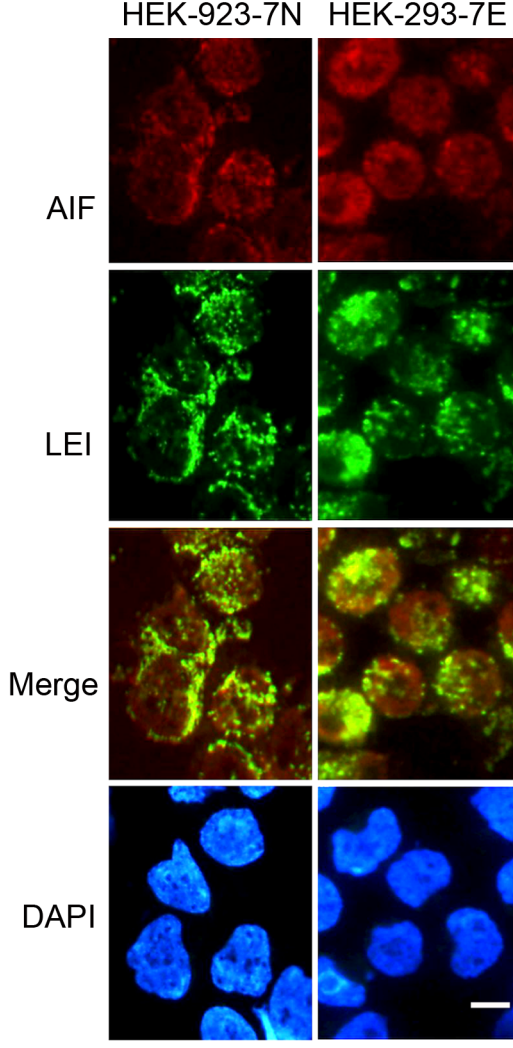
HEK-923-7N
HEK-293-7E
AIF
LEI
Merge
DAPI

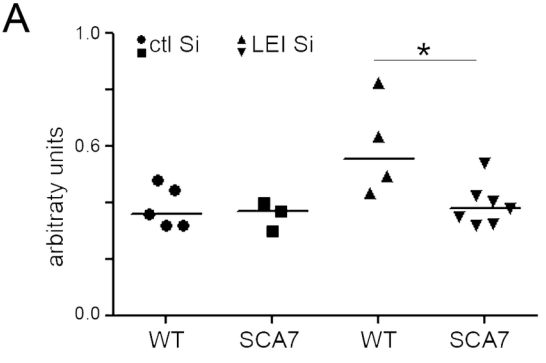
A
ctl Si
LEI Si
*
1.0
0.6
0.0
arbitraty units
WT
SCA7
WT
SCA7

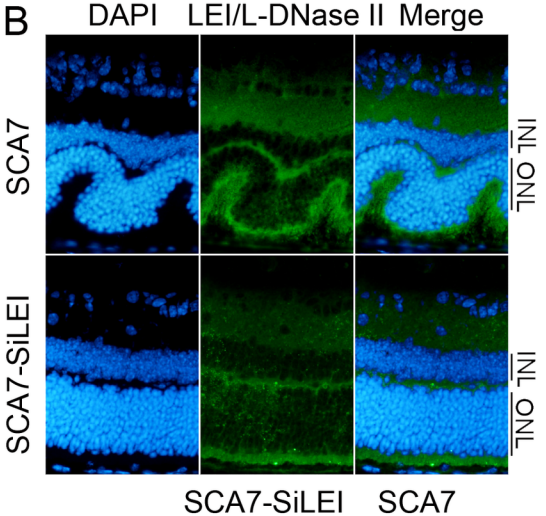
B
DAPI
LEI/L-DNase II
Merge
SCA7
SCA7-SiLEI
INL
ONL
INL
ONL

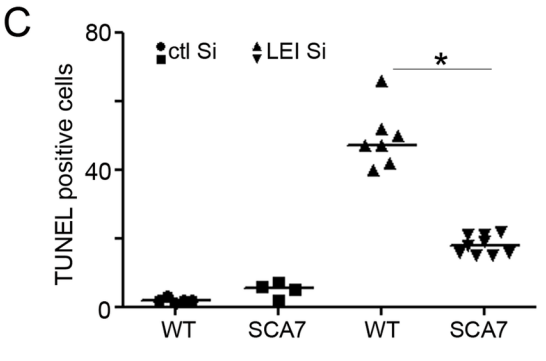
SCA7-SiLEI
SCA7
C
80
40
0
ctl Si
LEI Si
*
TUNEL positive cells
WT
SCA7
WT
SCA7

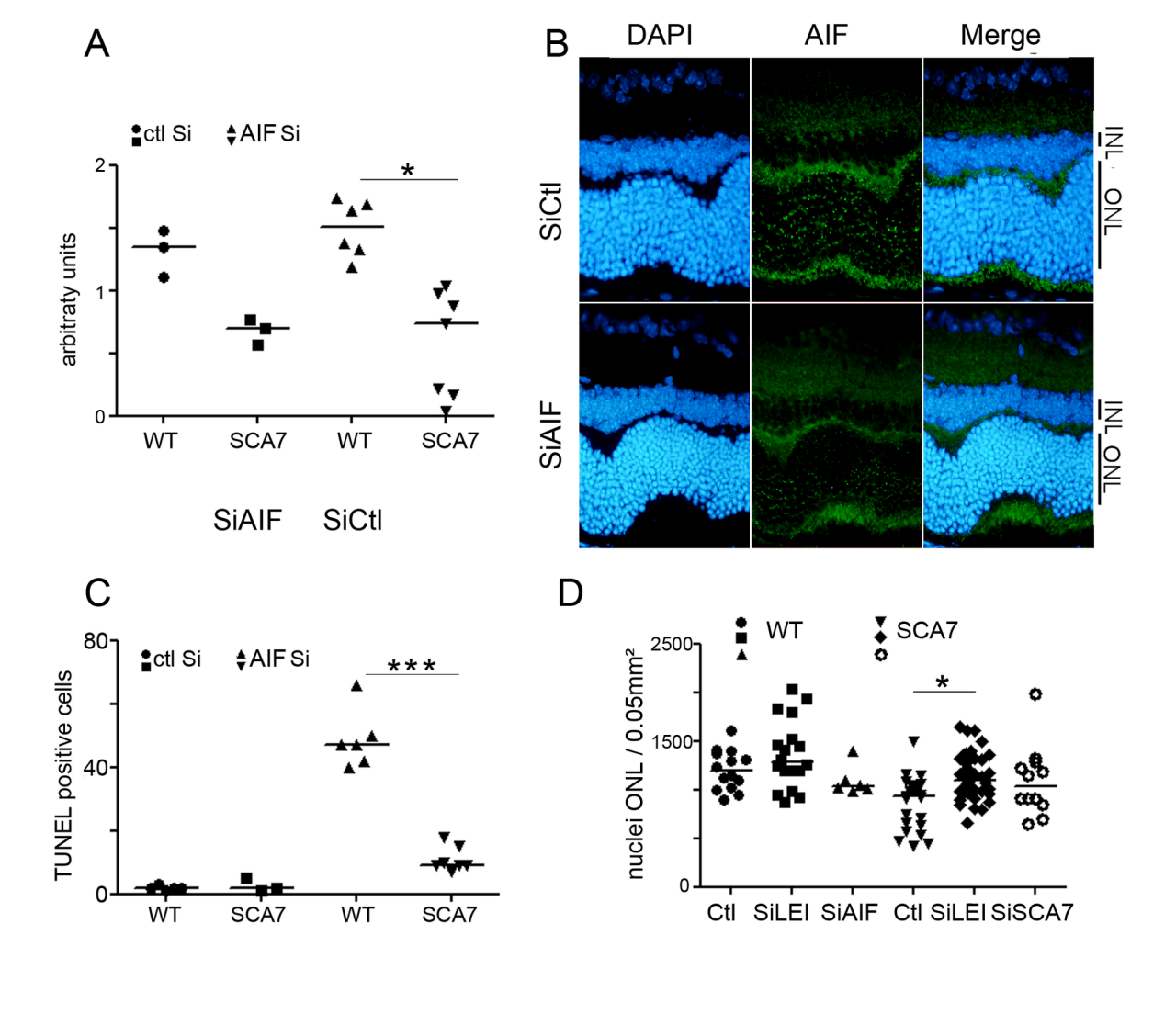
A
ctl Si
AIF Si
arbitraty units
2
1
0
*
WT
SCA7
WT
SCA7
SiAIF
SiCtl
B
DAPI
AIF
Merge
SiCtl
SiAIF
INL
ONL
INL
ONL
C
ctl Si
AIF Si
TUNEL positive cells
80
40
0
***
WT
SCA7
WT
SCA7
D
WT
SCA7
nuclei ONL / 0.05mm²
2500
1500
0
*
Ctl
SiLEI
SiAIF
Ctl
SiLEI
SiSCA7

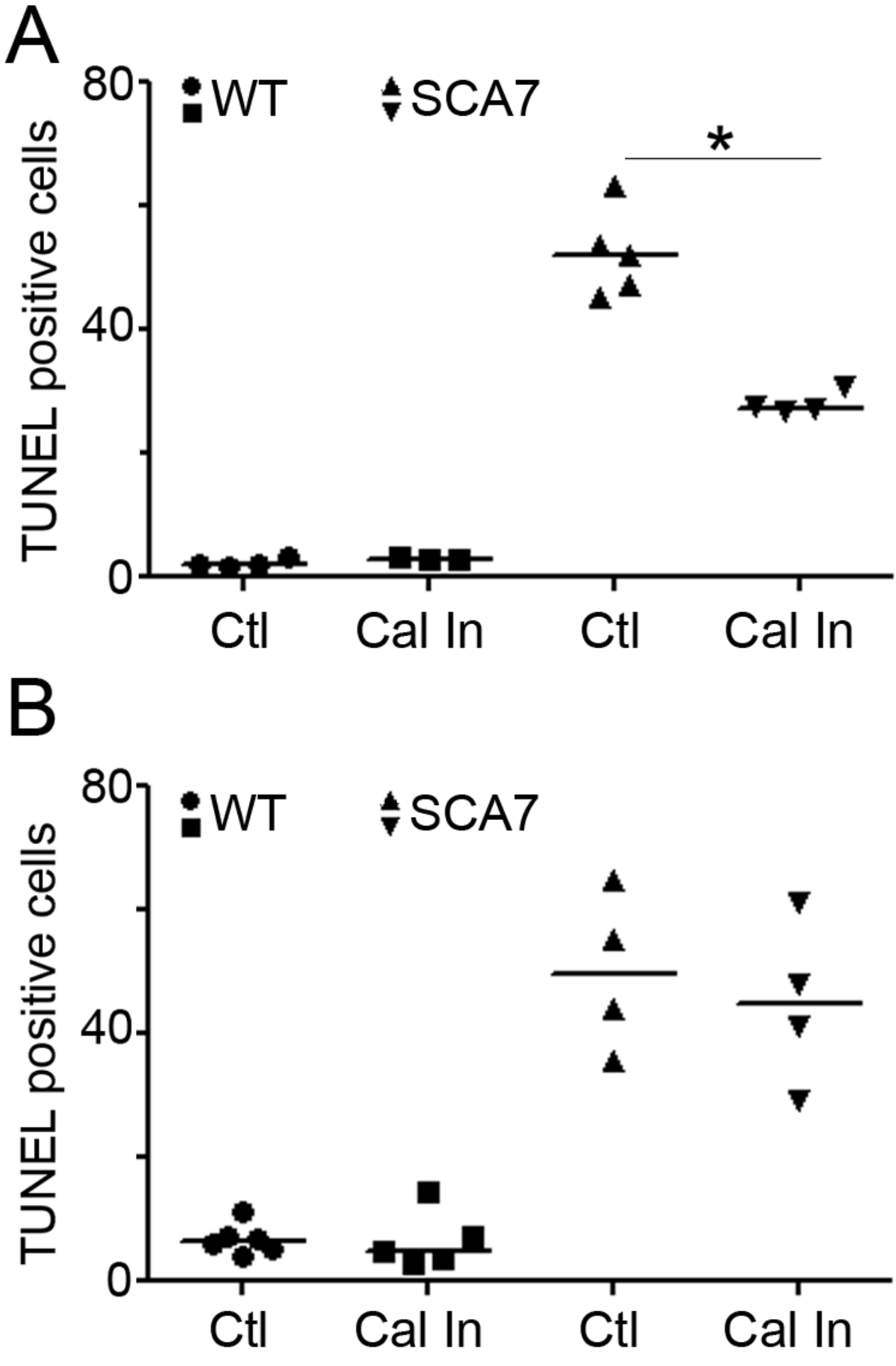
A
80
40
0
WT
SCA7
*
TUNEL positive cells
Ctl
Cal In
Ctl
Cal In
B
80
40
0
WT
SCA7
TUNEL positive cells
Ctl
Cal In
Ctl
Cal In